Research Article

Transportation Research Record
2026, Vol. 2680(2) 347–365

DOI: 10.1177/03611981251364837
journals.sagepub.com/home/trr

Typology of Bike Lane Users Motion on Horizontal Curves: A Surrogate Safety Approach

Morteza Hossein Sabbaghian[1], David Llopis-Castelló[1], and Alfredo García[1]

Abstract

This study examines the safety implications of horizontal curves in bike lanes, focusing on cyclists' and e-scooter riders' behavior. As cities transition from autocentric to sustainable transportation systems, bike lanes are increasingly integrated into urban infrastructure, particularly in Europe. Despite the benefits of active transportation, safety concerns for bike lane users persist. Horizontal curves can pose significant safety risks as a rest of lower radii, higher curvature degrees, and reduced surface friction. This study has shown that cyclists and e-scooter riders are significantly affected by sudden changes in geometry, reacting by aggressive maneuvers and increased risks of conflict and fall. To address this, a motion analysis methodology is proposed to identify risky maneuvers in bike lanes, using microscopic analysis of trajectory and speed, revealing naturalistic reactions of bike lane users to various curve geometries. The study employs previous track typology and density-based spatial clustering algorithms to cluster distinct trajectory patterns. Additionally, a decision tree regression model finds the degree of curvature as the most effective variable in user motion behavior. Findings indicate that horizontal curve geometry significantly influencing user behavior. Generally, left-turn maneuvers on curves show greater diversity and higher risks, especially in sharp curves on a bidirectional bike lane. Speed analysis reveals that reducing curve radii increases speeding behaviors and variance. The proposed method is scalable and can help in the development of mitigation strategies such as geometric treatments, surface skid resistance improvements, enhanced signage, and enforcement in high-risk curves identified after using this approach.

Keywords

bike lane safety, horizontal curve, micromobility behavior, trajectory, speed

Bike lanes are increasingly being incorporated into urban environments as part of a shift toward more sustainable and active transportation systems. European cities are at the forefront of this transition, implementing measures to slow city transport and reduce traffic crashes (*1*). Despite the benefits of active transportation—such as reduced congestion, noise, and pollution (*2*)—safety concerns for bike lane users persist, particularly for cyclists and e-scooter riders who are more vulnerable to conflicts because of their lower mass and higher exposure to impact compared with motor vehicles. Advances in motion data collection, including increased roadside cameras, autonomous vehicle data sets, and real-time object detection algorithms like YOLO (You Only Look Once), have improved traffic safety assessments (*3*). However, dedicated monitoring for bike lanes remains limited, with issues such as underreporting of crashes and insufficient data on single-bicycle crashes. The RECYCLIST tool introduced by Bjørnskau et al. (*4*) aims to address this data gap by enhancing crash registration for cyclists. Horizontal curves in bike lanes are particularly prone to conflicts. These curves can be classified into four types: first curves, isolated curves, reverse curves, and consecutive curves (*5*). Safety concerns arise as a result of lower radius, higher curvature, and reduced friction on some surfaces (*6*).

[1]Highway Engineering Research Group, Universitat Politècnica de València, Valencia, Spain

Corresponding Author:
Morteza Hossein Sabbaghian, mhossab@upv.es

As discussed in previous studies, the typology of a vehicle's trajectory primarily refers to the lateral positional relationship between the trajectory and the road's edge line or centerline. Many studies on vehicle motion analysis on road curves have utilized the lateral deviation (LD) between the trajectory and the centerline (*7–10*). Later, Xu et al. (11) introduced the LD rate of the trajectory, which accounts for the impact of lane width changes on curves (calculated as the lateral distance to the centerline divided by the road's cross-sectional width). However, on bike lanes, the bends are typically not widened, and lane width remains constant. Therefore, the fitted curve in this study, based on LD, can often be suitable for reconstructing the most accurate trajectory arc for bike lane curves (*11*).

Lane departure on horizontal curves is a leading cause of many side-swipe, rear-end, and single-vehicle run-off-road crashes for motor vehicles. In a study by Chen et al., a driving simulator was used to assess lane departure of motor vehicles on curves on a mountainous freeway in China. The findings indicated that both the horizontal curvature at the current segment and the difference (max.–min.) in horizontal curvature within the 300-m upstream alignment significantly increased the likelihood of lane departure of road users (*12*).

Unlike motor vehicles, cyclists and e-scooter riders, who have greater maneuverability and steering angles, are more affected by sudden changes in geometry and horizontal curvature (*13*). This issue is exacerbated in retrofitted bike lanes with inconsistent alignments and reduced traction. This study proposes a method to identify risky maneuvers at high resolution through microscopic trajectory analysis on isolated horizontal curves of bidirectional bike lanes, aiming to improve bike lane safety by revealing user responses to different curve geometries. The result of this research can be used for designing countermeasures such as geometric optimizations, surface treatments, and enhanced signage, with potential for further research in micromobility safety using the proposed segmentation approach.

Despite the distinct maneuvering dynamics of bike lane users compared with motor vehicles and the need for optimizing bike lanes accordingly, a review of the literature reveals that curve geometry optimization for bike lanes has received very little attention from researchers (*14*). In the following, these studies, including their methodologies and results, are first discussed. Next, previous attempts for pattern mining, classification (typology), and clustering of trajectory data are briefly explained, and the limitations of the current state-of-the-art are highlighted.

Optimization of Horizontal Curve Geometry

The Dutch design manual for bicycle traffic (CROW) outlines five key parameters for designing horizontal curves on bike lanes: route type (basic network/connection or main cycle route), design speed (12 km/h, 20 km/h, 30 km/h), minimum associated radius (5 m, 10 m, 20 m), minimum sight distance in motion (distance covering in 4–5 s), and stopping sight distance (40 m at 30 km/h; 21 m at 20 km/h). Additionally, it mandates an operational width for cyclists of 750 mm, with a 250 mm safety distance (clearance) for passing or overtaking cyclists. The safety distance is set for the conditions in which cyclists are forced to ride slower than 15 km/h because of factors like swaying motion, crosswinds, and so may have an LD of 200 mm under normal conditions (*15*).

A relevant study on horizontal curve optimization for bike lanes was conducted by Ul-Abdin et al. (*16*). This research revealed that to determine an optimal radius of curvature and widening value on bike lane curves, imposed forces and human factors specific to all micromobility users must be taken into account. This is because bike lane users make riding decisions based on the forces they experience and their perceptions of the path ahead (*16*). The study proposed an optimized bike lane design system using theoretical trigonometric derivations. They calculated the optimal radius of curvature, accounting for centrifugal, centripetal, and gyroscopic forces on users, while considering variations in the radius of curvature depending on the location of the center of gravity: whether it is on the cyclists themselves, on the bicycle, or on the connection point between cyclists and the road surface (*16*).

A previous study by the authors analyzed micromobility user displacement on curved bike lanes, showing that left-turning users, especially scooter riders, were more likely to veer into the opposite lane, increasing conflict risks. However, since user typology was not considered in that study, the current research extends this work by incorporating user classification to provide a more comprehensive understanding of micromobility behavior (*17*). Other studies have primarily focused on modeling and optimizing the deceleration and behavior of professional users themselves (e.g., racing cyclists) rather than on curve design (*18*, *19*).

Trajectory Data Mining

With advancements in global positioning systems (GPS) and emerging automated vehicles, more GPS-based trajectory data are now available for mobility analysis, which has spurred increased research in data mining techniques and computer science. Yet, there are still challenges such as low frequency of positioning data, high power consumption, and personal privacy concerns that are discussed in the literature. According to Shen et al. (*20*), current applications of large-scale trajectory data include traffic jam detection, automatic driving, navigation route planning, and mobility modeling.

For micromobility, however, there is less data available since these personal devices are often not equipped with GPS or sensors. Few studies on shared micromobility have utilized GPS data, primarily for generating trip trajectories at a resolution insufficient for safety assessment and more suited for routing analysis. For example, Zakhem and Smith-Colin (*21*) conducted an analysis of heavily used corridors to optimize parking. Pellicer-Chenoll et al. (*22*) analyzed gender differences in the use of Valencia's Bicycle Sharing System (BSS) by examining over 5.3 million trips over 4 years. The findings reveal that women use BSS less frequently than men, avoid peripheral areas at night, and exhibit different network density and centrality patterns (*22*). Another similar study examines how gender, age, and parenthood influence the travel behavior of bike-share cyclists and private e-scooter riders in Barcelona using GPS-tracked trips and a multilevel linear mixed effects model. The findings reveal a significant gender speed gap among e-scooter users, influenced by urban design and social factors, highlighting the need for intersectional approaches in micromobility research and policy-making (*23*).

Other sources of data used in previous studies for generating trajectory of bike users include video recordings (*24*) and autonomous vehicles data (*25*) when interacting with bike lane users. Notably, Sanjurjo-de-No et al. (*26*) examined gender differences in micromobility usage, finding that men tend to ride faster while women position themselves farther from motorized traffic, highlighting the importance of gender-inclusive urban planning for safer infrastructure (*26*).

Trajectory Classification and Clustering

There are no studies in the literature yet that classify the trajectory behavior of bike lane users on horizontal curves. However, some observational studies have addressed this for road users. For instance, Spacek (*27*) identified six types of track paths and their characteristics along curves. Subsequent research has applied these classifications to evaluate vehicle trajectories on various horizontal curves, such as those on mountainous roads (*28*), combined alignments (*12*), and simulated two-lane rural highways (*29*).

To gain deeper insights into user behavior and enhance microsimulation models, researchers employed clustering methods to categorize user maneuvers. The *k*-means algorithm, introduced by MacQueen (*30*) and refined by Hartigan and Wong (*31*), is a popular method that minimizes the distance between data points and their assigned cluster centroids. This iterative process continues until convergence. Similarly, the DBSCAN (Density-Based Spatial Clustering of Applications with Noise) algorithm, developed by Xu et al. (*32*), identifies clusters of varying shapes and sizes based on density, making it particularly effective for distinguishing distinct trajectory patterns in user behavior.

In 2002, model-based clustering and classification emerged, integrating hierarchical clustering, the expectation-maximization (EM) algorithm for mixture models, and Bayesian Information Criterion (*33*). The EM algorithm involves calculating the likelihood of observations belonging to clusters and updating parameter estimates iteratively. Clusters are modeled using Gaussian distributions with maximum-likelihood values. Following clustering, the *K*-nearest neighbors method classifies the clusters. More advanced flexible fitting models like Locally Weighted Regression (*34*), Multivariate Adaptive Regression Splines (*35*), Kernel Support Vector Machines (*36*), Bayesian Regularized Neural Networks (*37*), and Gaussian Processes (GP) (*38*) have been developed, offering superior fit over conventional models but with less interpretability. Mohammed et al. (*39*) applied the GP method to analyze cyclist behavior, using a multivariate finite mixture model to categorize maneuvers during following and overtaking interactions. They grouped maneuvers into initiation, merging, and postovertaking states, utilizing longitudinal distance, lateral distance, and speed difference data collected via computer vision and video data.

Survey-Based Risk Perception Studies

A common area of study in micromobility safety research is users' risk perception, often assessed through survey studies. However, these studies are typically broad, not focused on specific bike lane segments, and rarely combined with field observations or track tests. Despite these limitations, they provide valuable insights into general trends and gender impact.

For example, Prati et al. (*40*) examined gender differences in cycling attitudes, infrastructure preferences, risk perception, and crash exposure among regular cyclists across six European countries. The study found that while gender differences in cycling attitudes were minimal, women reported higher discomfort in mixed traffic, greater risk perception, and lower exposure to severe crashes compared with men. This highlights the influence of gender norms on cycling behavior (*40*). Another study designs surveys to explore risk-taking behaviors among e-scooter users in Paris, focusing on factors such as alcohol, drug consumption, and smartphone use while riding.

The results indicate that younger, male, and frequent e-scooter riders are more likely to engage in risky behaviors, with longer trips also being linked to increased risk (*41*).

Objective

The primary gap identified in the literature review is the lack of analysis of the microscopic behavior of bike lane users on curves. This analysis is crucial to ensure that bike lane geometry is navigable and does not prompt aggressive maneuvers, which could heighten the risk of instability and conflicts. Existing studies that examine users' trajectories predominantly focus on the risk of conflicts with motor vehicles at intersections, rather than conflicts between bike lane users themselves. Therefore, this study aims to address this gap by introducing a novel method for high-resolution assessment of user motion, enabling the investigation of the typologies of curving maneuvers among micromobility users, both cyclists and e-scooter riders. As the primary objective is to observe users' responses to various curve geometries, data collection will be conducted under optimal environmental conditions (dry pavement and daylight) to eliminate external factors that could increase instability.

Methods

The methodology proposed for this study comprises six key components: (1) geometric data collection, (2) site selection, (3) video recording, (4) motion data extraction, (5) track classification and descriptive analysis of speeds, and (6) clustering analysis and decision tree modeling. Nine isolated horizontal curve sites are selected after analyzing over 30 horizontal curves in high-traffic areas across Valencia. To ensure diversity, the city is divided into four main zones (North-East, North-West, South-East, South-West), allowing for a representative selection from different regions. The curves are chosen with particular attention to their geometric diversity, especially their radius, covering a wide range from very sharp curves (2 m) to very flat ones (78 m), including intermediate values. Notably, two curve sites with a 5-m radius are selected, as this is the minimum recommended radius for bike lane bends according to guidelines such as CROW.

The minimum sample size for precision is estimated using normal distribution theory or power analysis concepts, based on a similar study in Valencia by Cabrera and Sofía (*42*) involving large-sample data on the characterization of micromobility users' meeting maneuvers. Assuming a maximum error of 5 cm and an LD of 25 cm, the minimum required number of users per site is 96. Therefore, a sample size of 100 users per site is set to ensure sufficient precision. In this section, the methods for the selection, collection, and extraction of data are explained, as well as the methods used for modeling and analysis.

Geometric Data Collection and Site Selection

Three criteria were established for selecting a representative sample of isolated horizontal curves: geometric diversity, spatial distribution, and traffic volume adequacy. Geometric diversity and spatial distribution ensure that the sample represents a variety of geometries and locations across the city of Valencia, Spain, while traffic volume adequacy is important for minimizing the time required to collect motion data. To meet these criteria, the process begins with identifying, labeling, and mapping over 30 horizontal curves in Valencia using Google Maps. The spatial distribution of these curves across different city areas (North, South, West, East) was carefully considered. Subsequently, the alignment creation tool in Autodesk Civil 3D, along with high-resolution orthophoto maps from PNOA (Plan Nacional de Ortofotografía Aérea) (*43*), were utilized to recreate and extract the geometries of the initial sample. This approach aims to reduce the sample size while ensuring it meets the established criteria for geometric diversity, spatial distribution, and traffic volume adequacy. Each curve site selected for this study possesses a distinct radius and degree of curvature, both of which are automatically computed and extracted from the bike lane centerline alignment using Civil3D software. The radii of the nine selected curves range from 2 to 78 m (6.56 ft to 255.91 ft), and the degrees of curvature vary from as sharp as 769 degrees to as flat as 22 degrees (Figure 1). Table 1 summarizes all selected sites, including their label (e.g., third site in Northeast: NE3), bike lane type: two-way protected bike lane and nonprotected bike lane on the sidewalk, and five geometric characteristics.

The main geometric parameters of a simple isolated curve used in this study are illustrated in color in Figure 2. The red arc represents the arc length, the green line shows the chord length, and the blue line indicates the radius. The angle between the radii perpendicular to the back and forward tangents at PC and PT is the deflection angle (ã). The curve's sharpness, or degree of curvature (degrees), can be calculated using Equation 1 as follows:

$$D = \frac{180}{\pi . R} \tag{1}$$

Video Recording

Collecting naturalistic data requires specific techniques and considerations to avoid users detecting the camera, ensure a proper angle of the camera view, and ensure

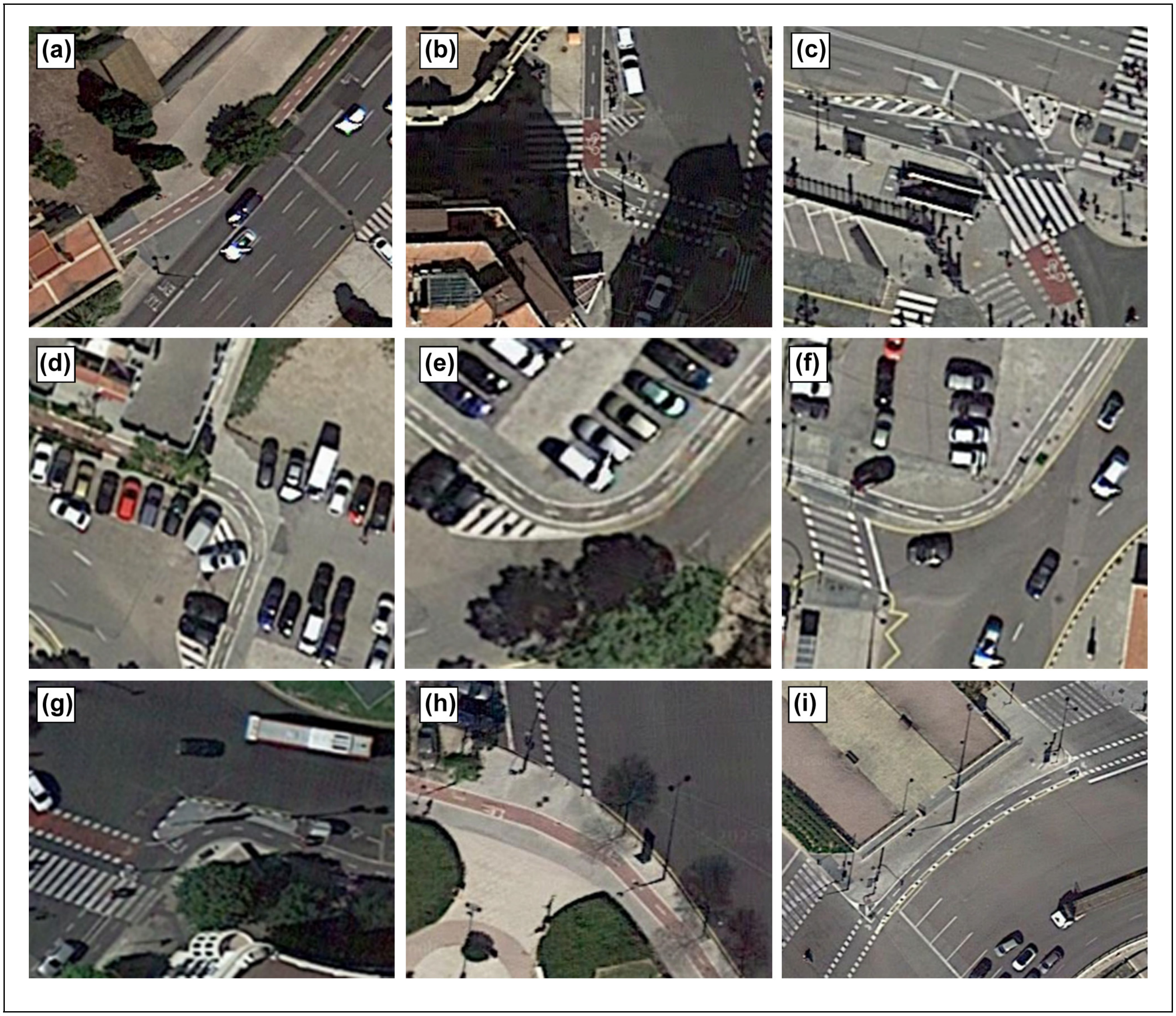

Figure 1. Bird's-eye view of the nine selected isolated curve sites: (*a*) NW1 (*44*), (*b*) SW1 (*45*), (*c*) SW3 (*46*), (*d*) NE3 (*47*), (e) NE9 (*48*), (*f*) NE8 (*49*), (*g*) SW2 (*50*), (*h*) SE4 (*51*), (*i*) SE3 (*52*).
(*a*) NW1 (R1 = 2 m).
(*b*) SW1 (R2 = 5 m).
(*c*) SW3 (R3 = 5 m).
(*d*) NE3 (R4 = 6 m).
(e) NE9 (R5 = 7 m).
(*f*) NE8 (R6 = 9 m).
(*g*) SW2 (R7 = 10 m).
(*h*) SE4 (R8 = 22 m).
(*i*) SE3 (R9 = 78 m).
Note: PC = point of curve; PI = point of intersection; PT = point of tangency.

recordings are saved properly and stored in a secure online platform. For this study, a 6-m tripod and Garmin Virb cameras were used for each day of data collection. These compact cameras (32 × 53 × 111 mm) with wide lenses offer 1080p HD recording, a 16-megapixel CMOS image processor, Bluetooth connectivity for live remote monitoring, and can be unnoticed because of their size. To keep the camera concealed from users, the tripod was placed at a minimum lateral distance of 10 m or more from the outer edge of the horizontal curve at the measurement point. If this distance is not feasible, the tripod can be positioned near one of the tangents with a

Table 1. Isolated Curve Sites Geometric Parameters

#	Site	Type	Length, m (ft)	Radius, m (ft)	Deflection angle (d)	Chord length, m (ft)	Degree of curvature (d)
R1	NW1	Nonprotected	4 (13.12)	2 (6.56)	89	3.2 (10.50)	769
R2	SW1	Protected	6 (19.69)	5 (16.40)	71	5.9 (19.36)	341
R3	SW3	Protected	4 (13.12)	5 (16.40)	46	4.0 (13.12)	341
R4	NE3	Nonprotected	10 (32.81)	6 (19.69)	89	8.8 (28.87)	278
R5	NE9	Nonprotected	11 (36.09)	7 (22.97)	84	9.8 (32.15)	240
R6	NE8	Nonprotected	13 (42.65)	9 (29.53)	85	11.8 (38.71)	200
R7	SW2	Protected	12 (39.37)	10 (32.81)	69	11.1 (36.42)	178
R8	SE4	Nonprotected	13 (42.65)	22 (72.18)	33	12.7 (41.67)	78
R9	SE3	Protected	37 (121.39)	78 (255.91)	27	36.9 (121.06)	22

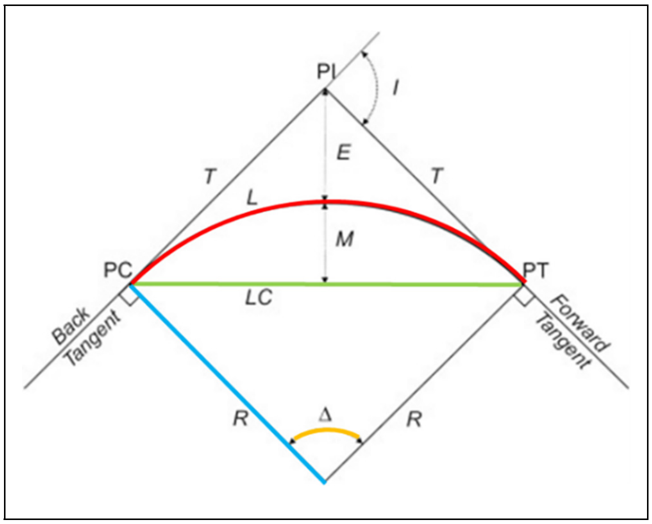

Figure 2. Geometric parameters of a simple isolated curve (*15*).
Note: PC = point of curve; PI = point of intersection; PT = point of tangency.

minimum lateral offset equal to the width of the bike lane or 2 m. Continuous monitoring of users' gaze and head movements is essential to ensure they are unaware of the recording. Users who notice the camera should be excluded from data extraction. If an increasing number of users detect the camera, the tripod's location must be adjusted. The ideal camera angle for motion studies is a bird's-eye view, but this is often impractical for naturalistic studies as a result of restrictions on drone usage in urban areas or the need for proximity to the bike lane edge. Consequently, for this study, the camera was mounted on a 6-m extendable tripod at a 90-degree angle from the vertical axis. When the lateral distance was insufficient, the camera was tilted downward (up to 45 degrees) to capture the entire horizontal curve.

Data collection took place over 4 months (September 2023 to December 2023), starting during the morning and evening peak hours (8:00 a.m. and 2:00 p.m.) and continuing for up to 4 h per round or until 25 users per direction and per user type were observed, totaling 100 users at each site. The goal was to observe passing users under free-riding conditions while ensuring sufficient traffic to minimize data collection time. Daytime and dry conditions were chosen to focus solely on studying the impact of geometry under normal environmental conditions. Moreover, only users (cyclists and e-scooter riders) navigating the curve under free-flow conditions were counted. This means that, during their navigation, there were no users directly in front or in the opposite lane who could interact with or impact the behavior of the observed user, as well as pedestrians close to the lane. Figure 3 shows the two camera placement setups used in this study. In the first setup (a), the camera is placed near the point of intersection outside the curve, positioned to capture the entire curve while remaining far enough away to avoid attracting users' attention. This was observed to be the most effective location for recording naturalistic user behavior without them noticing. When this placement was not feasible because of land use or limited space, the second setup (b) positioned the camera near one of the tangents, ideally behind obstacles to stay as unobtrusive as possible. In this case, user gaze was monitored, and those who noticed the camera were excluded from the analysis.

Motion Data Extraction

Before initiating the data extraction process, it is necessary to define two critical preprocessing elements: (1) a proper lateral segmentation of the bike lane (Figure 4) to enable microscopic risk assessment, and (2) an understanding of the typology of possible track patterns generated by bike lane users. The latter can initially be adopted from previous studies on the track typology of motor vehicles on curves.

The observation area for user trajectory and speed extends beyond the confines of the bike lanes to include adjacent regions, particularly where bike lanes are integrated with pedestrian walkways. The typical width of the bike lanes analyzed in this study is 2.0 m (5.56 ft) with markings and 1.7 m (5.58 ft) without markings. For

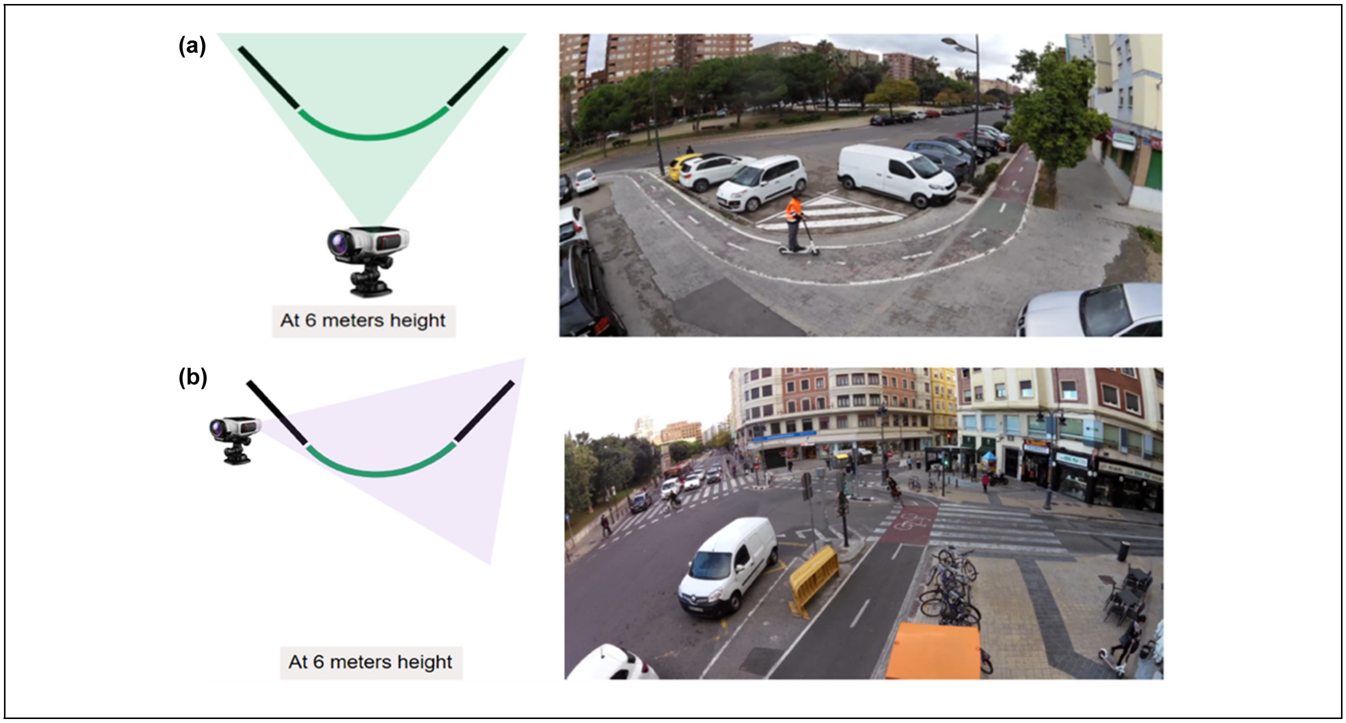

Figure 3. Tripod placed at two setups: (*a*) near point of intersection (NE3) and (*b*) near tangent (SW1).

segmentation, the curve of the bike lane is initially divided into three sections of interest: Point of Curvature (PC), Midpoint (MP), and Point of Tangency (PT). Additionally, four cross-sectional regions are delineated as shown in Figure 4:

1. Lane (LN): The user's wheel is positioned within the lane, extending from the right edge to 52.5 cm (1.722 ft) toward the central marking.
2. Central Marking (CL): The user's wheel is positioned on or within 52.5 cm (1.722 ft) to the right of the central marking, which accounts for half of the operational width (37.5 cm or 1.23 ft) and the marking width (10 cm or 0.328 ft) combined (totaling 47.5 cm or 1.56 ft). This positioning poses a risk of crossing conflicts with users traveling in the opposite direction.
3. Opposite Lane (OPL): Users breach their designated lane, causing their wheel to enter the lane for opposite direction travel (in bidirectional bike lanes), thereby increasing the risk of head-on and side-angled conflicts.
4. Out of Lane (OTL): This area is to the right of the user's movement direction but outside the bike lane, where interactions with pedestrians or collisions with fixed objects can occur.

After segmentation, the maneuvers of bike lane users were classified by adopting six track types from motor vehicle dynamics research on horizontal curves (Figure 5) (*27*). The first track is the Ideal Behavior (ID) or the optimal track, characterized by a symmetrical path along the

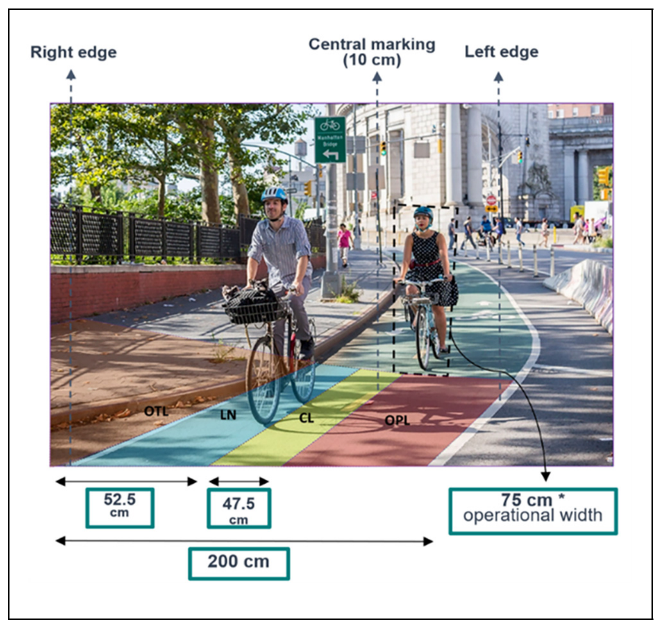

Figure 4. Regions of interest for identifying user's position on the curve with users making a right-turn; background image source (*53*).

Note: OTL = out of lane; LN = lane; CL = central marking; OPL = opposite lane.

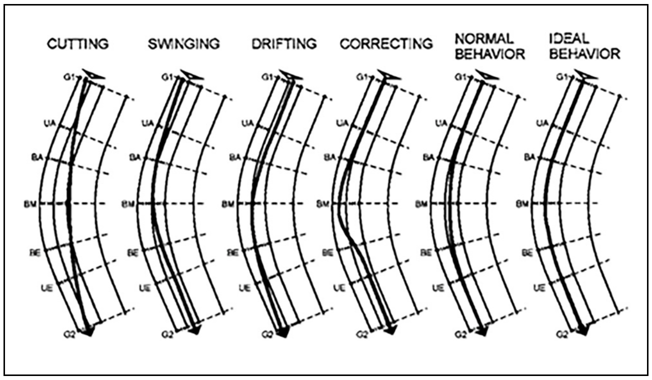

Figure 5. Six track types for motor vehicle maneuvers on horizontal curves (*27*).
Main curve points:

- G1: Start of entering tangent
- UA: Beginning of transition curve (clothoid)
- BA: Beginning of circular arc (SC)
- BM: Middle of circular arc
- BE: End of circular arc (CS)
- UE: End of transition curve (clothoid)
- G2: End of exit tangent

center of the dedicated lane in each direction. This behavior indicates maximum stability and minimal deviation, promoting consistent and predictable movement within a narrow central area of the bike lane. Users following this track type demonstrate the most efficient use of the lane, enhancing overall safety and fluidity in traffic flow. Normal Behavior (NR) also indicates a symmetrical track along the center but allows for a broader area of movement. This type accommodates slight deviations (minor cutting) toward the curve's inside, without encroaching on the centerline. Both ID and NR behaviors translate into a reliable and secure riding path, emphasizing minimal deviation from the initial path and ensuring a stable riding experience. More complex behaviors previously found include Correcting (CR), Cutting (CT), Swinging (SW), and Drifting (DR). The Correcting (CR) behavior involves an S-shaped path where users initially drift toward the curve's outside before correcting their steering midway through, often attributed to an underestimation of the curve's length or sharpness. This behavior reflects the users' adjustments to unexpected curve characteristics. Cutting (CT) behavior involves deliberate, strong cutting to the inside of the curve, representing a conscious effort to balance centrifugal forces. Cyclists exhibiting this behavior are making calculated adjustments to maintain stability and control, which can be influenced by their speed and familiarity with the route. Swinging (SW) and Drifting (DR) both describe asymmetrical track paths but in opposite manners. Swinging (SW) behavior sees cyclists start on the right side of the lane and drift left toward the curve's end, while Drifting (DR) involves starting on the left and drifting right. The combination of the discussed track types with four lateral segments resulted in 28 distinct track-segment classes.

Table 2. Acronyms for Classifying Maneuvers by Track Type and Lateral Segment

#	Acronym	Track type_lateral segment
1	ID_LN	Ideal_Lane
2	ID_CL	Ideal_Central Marking
3	ID_OPL	Ideal_Opposite Lane
4	ID_OTL	Ideal_Out of Lane
5	NR_LN	Normal_Lane
6	NR_CL	Normal_Central Marking
7	NR_OPL	Normal_Opposite Lane
8	NR_OTL	Normal_Out of Lane
9	CR_LN	Correcting_Lane
10	CR_CL	Correcting_Central Marking
11	CR_OPL	Correcting_Opposite Lane
12	CR_OTL	Correcting_Out of Lane
13	DR_LN	Drifting_Lane
14	DR_CL	Drifting_Central Marking
15	DR_OPL	Drifting_Opposite Lane
16	DR_OTL	Drifting_Out of Lane
17	SW_LN	Swinging_Lane
18	SW_CL	Swinging_Central Marking
19	SW_OPL	Swinging_Opposite Lane
20	SW_OTL	Swinging_Out of Lane
21	CT_LN	Cutting_Lane
22	CT_CL	Cutting_Central Marking
23	CT_OPL	Cutting_Opposite Lane
24	CT_OTL	Cutting_Out of Lane
25	UN_LN	Unclassified_Lane
26	UN_CL	Unclassified_Central Marking
27	UN_OPL	Unclassified_Opposite Lane
28	UN_OTL	Unclassified_Out of Lane

Finally, the motion analysis software Kinovea (version 9.5) was utilized to extract users' spatiotemporal data from the video recordings. These data include wheel positions (lateral offsets from the centerline) and spot speeds at the three sections of PC, MP, and PT, as well as timestamps and distances between these sections. The instantaneous speeds (average segmental speed) are retrieved to validate the spot speeds at the sections of interest.

Track Classification and Descriptive Analysis of Speeds

The data extracted from the previous step is organized into two distinct Excel files for subsequent analysis. For the classification process, which involves grouping entities into predefined categories (*54*), 28 unique track typologies are synthesized from predefined track types and lateral regions (Table 2). Each typology is recorded in a separate row within the Excel file. For instance, a designation such as "CR-OPL" indicates a Correcting track type intersecting with the Opposite Lane region. The classification file columns capture the frequency of each

```python
import pandas as pd
import seaborn as sns
import matplotlib.pyplot as plt
import matplotlib.colors as mcolors

# Load the dataset from the CSV file
file_path = 'heatmap tracks.csv'
data = pd.read_csv(file_path, index_col=0)

# Define a diverging colormap from light blue to light grey to dark red
cmap = mcolors.LinearSegmentedColormap.from_list("diverging_blue_grey_red", ["lightblue", "lightgrey", "darkred"])

# Create the heatmap with the diverging colormap
plt.figure(figsize=(15, 10))
sns.heatmap(data, cmap=cmap, annot=False, cbar=True, linecolor='white', linewidths=0.5, center=0)
plt.title('Heatmap of Dataset')
plt.xlabel('Columns')
plt.ylabel('Rows')
# Save the plot as a PNG file with 300 DPI
plt.savefig('heatmap_output.png', dpi=300, bbox_inches='tight')

plt.show()
```

Figure 6. Python script for track typology heatmap generation.

track type at various curve sites, categorized by turn direction and user type. Column headings are explicitly labeled, such as "R1 LT-B," denoting a specific curve site (R1), a left turn (LT), and data related to bike users (B). This structured data is then used in a Python script to generate a heatmap visualizing the distribution of track types across curve sites with varying geometric properties, such as radius and degree of curvature. As shown in Figure 6, the script utilizes the seaborn and matplotlib libraries, employing a custom diverging colormap from light blue-grey to dark red to highlight track variations. Additional pie charts are created to provide a detailed breakdown of track typology at each curve site, categorized by turn direction and user type.

In this study, descriptive analysis of speed is performed at three critical sections—PC, MP, and PT—using JASP. The aim is to summarize speed data, including measures such as mean, median, standard deviation, 85th percentile speed, and minimum/maximum range at each section. These metrics help in understanding the overall performance, consistency, and safety considerations at each section of the bike lane by looking at speed variability and extremes. The analysis is first categorized by curve site, differentiated by radius, to examine how speed varies across curves with different geometric properties. This allows for an assessment of how curvature affects cycling and riding speed. Additionally, the data are analyzed based on user type and turn direction, providing insights into how these factors influence speed at each section. This approach enables a detailed understanding of speed variations as influenced by both geometric characteristics and user-specific variables.

Track Clustering and Decision Tree Model

For the clustering of tracks, there is no need for a predefined formatting, as the aim is to identify and validate the typologies adopted in classification. Therefore, the associated Excel file data set includes only the lateral offset distances from the centerline of the bike lane at the three sections of PC, MP, and PT, denoted as d-PC, d-MP, and d-PT. Clustering is the process of dividing these large collection of lateral offset values into smaller groups based on their similarity, without predefined classes (*54*). There are several types of clustering techniques, including K-Means Clustering, Hierarchical Clustering, Prototype-based clustering, Density clustering, and Model-based clustering. Clustering techniques can also be classified based on the algorithmic approach used to find clusters in the data set. The different types of clusters include exclusive or strict partitioning clusters, overlapping clusters, hierarchical clusters, and fuzzy or probabilistic clusters (*54*).

In this research, the objective is to identify patterns in the lateral offsets of users across different sections (d-PC, d-MP, d-PT) on a curve. The analysis began with the loading and normalization of the data set. The DBSCAN algorithm was chosen for clustering because of its ability to identify clusters of arbitrary shape and its robustness to noise and outliers.

Results

The examination of users' speed, along with the prevalence and characteristics of their track types during curve navigation, has provided important insights into cyclists' and riders' curving behavior and its safety implications. As described in the Methodology section, a descriptive analysis of speed was conducted, and classification, clustering, and a predictive model were developed. The results of these analyses and their implications are presented in this section.

Speed Analysis

The results of the descriptive analysis conducted using JASP software (version 18.3) are presented in four

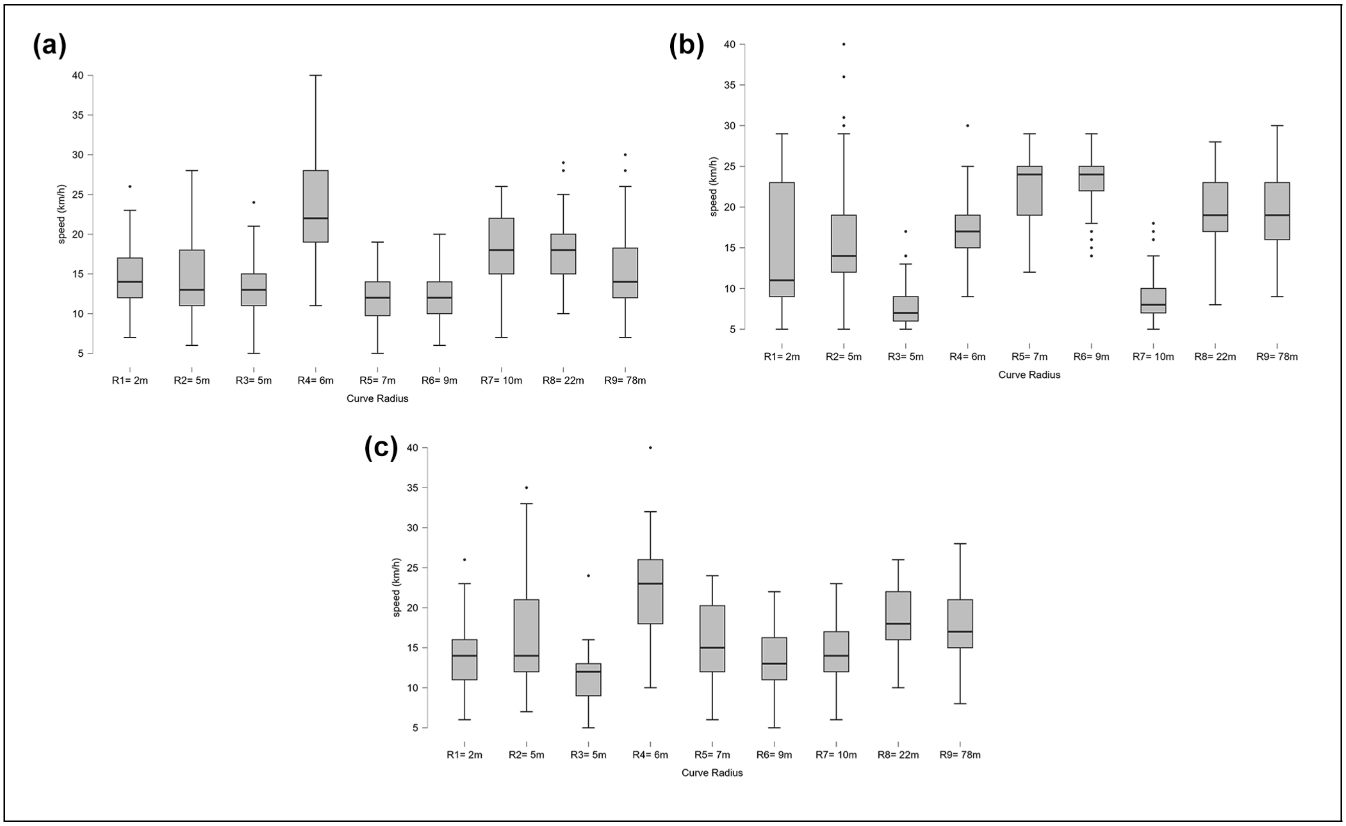

Figure 7. Box whisker plots of speed data for different radii for curve R1–R9: (*a*) Point of curvature, (*b*) Midpoint, and (*c*) Point of tangency.
Note: LT = left turn; RT = right turn.

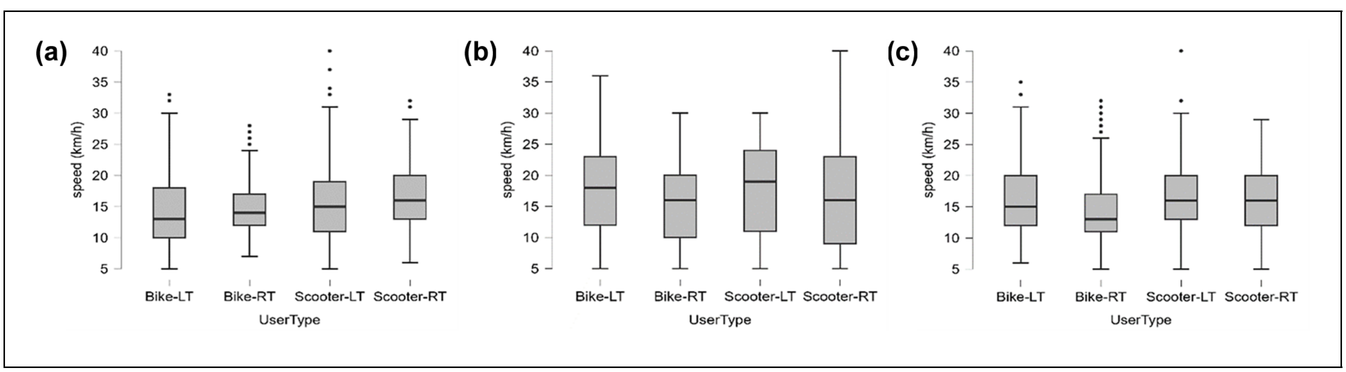

Figure 8. Box–whisker plots of speed data for each user type and direction for curve R1–R9: (*a*) Point of curvature, (*b*) Midpoint, and (*c*) Point of tangency.
Note: LT = left turn; RT = right turn.

box–whisker plots, as illustrated in Figures 7 to 10. These plots facilitate the observation of speed variations influenced by curve geometry, user type, and turn direction. The speed displayed on the vertical axis in all plots ranges from 5 km/h to 40 km/h (approximately 3.11 mph to 24.85 mph).

Figure 7 shows the impact of geometry on speed for sites R1 to R9, ordered by increasing radius. At MP, where most speeding (above the 15–20 km/h limit) occurs, speeding spikes after radii of 5 m and 10 m. The greatest speed dispersion appears at the sharpest radius (2 m), indicating that sharper curves lead to unpredictable speed

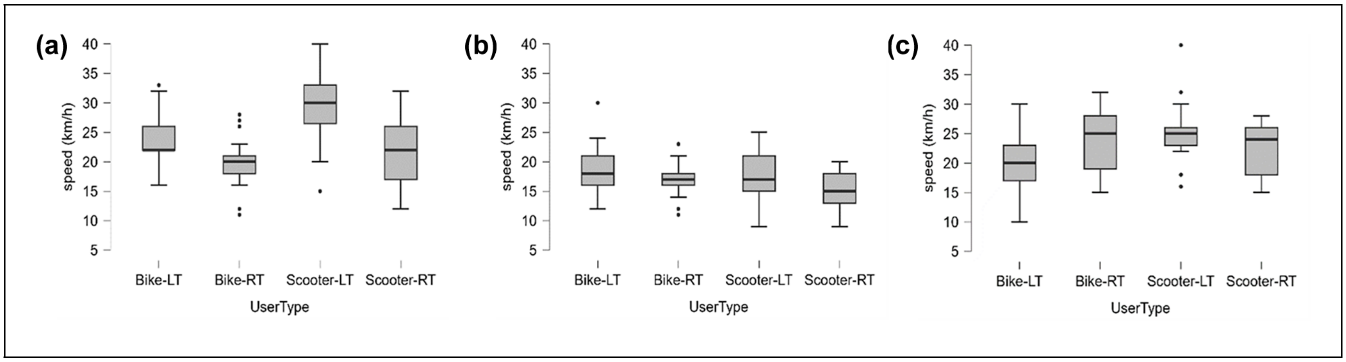

Figure 9. Box–whisker plots of speed data for each user type and direction for curve R4 = 6 m: (*a*) Point of curvature, (*b*) Midpoint, and (*c*) Point of tangency.
Note: LT = left turn; RT = right turn.

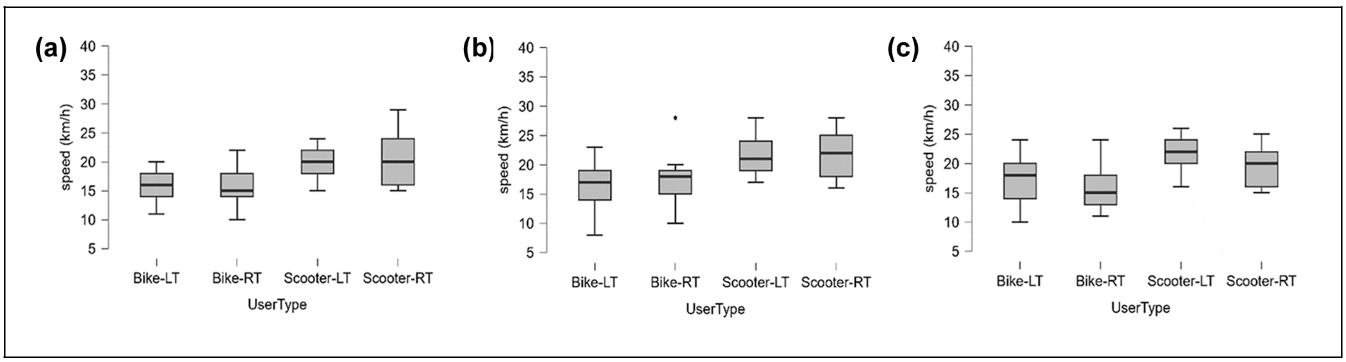

Figure 10. Box–whisker plots of speed data for each user type and direction for curve R8 = 22 m: (*a*) Point of curvature, (*b*) Midpoint, and (*c*) Point of tangency.
Note: LT = left turn; RT = right turn.

patterns and decreased adherence to the path. For PC, speeds stay below 20 km/h at the lowest radius, but users tend to accelerate through the curve at MP, raising risks of instability, falls, or conflicts with oncoming users. On flatter curves (22 m and 78 m) and some sharper ones (2 m, 7 m, 9 m), speeds increase on MP. This pattern, suggesting maneuvers that diverge from curve alignment, will be further examined in the track typology section.

Another pattern is that for sharp curves with radii below 10 m, the data show more outliers and varied patterns. For instance, although sites R2 and R3 both have a 5 m radius and are classified as protected types, their speed patterns differ. R2, with a 71-degree deflection angle, shows greater speed variation and increasing speeds throughout the curve. In contrast, R3, with a 46-degree deflection, follows the expected pattern of speed reduction at the MP and an increase at the PT. Each plot includes an orange highlight indicating Valencia's speed limit range, from 15 km/h to 20 km/h (9.32 mph to 12.43 mph)—the higher limit for protected sidepaths and the lower for nonprotected paths on sidewalks where pedestrians are present.

Figure 8 combines speed data from curve sites R1–R9 to compare the effects of user type and direction. E-scooters show the highest speeds and variability for both left and right turns at the MP. Comparing left to right turns for both e-scooters and bikes, the median speed is generally lower for right turns at MP and PT, but increases on PC for right turns. Since Figure 8 combines data from various geometries, it may introduce bias when assessing the effect of geometry in comparisons between user types and directions. To address this, two example series of box–whisker plots (Figures 8 and 9) were created, representing a sharp curve (R = 6 m) and a flat curve (R = 22 m).

Figures 9 and 10 illustrate that on sharper curves, all users tend to exceed speeds of 20 km/h on both the entry (PC) and exit (PT) tangents. In contrast, on flatter curves, only e-scooter users exhibit this behavior, and at lower speeds. Additionally, e-scooters generally have higher median speeds on left turns than right turns across both curve types. For bike users, this trend is evident only on sharper curves at the entry (PC) and midpoint (MP) of the turn, while the opposite trend appears at the exit (PT), aligning with the mixed-pattern trends observed in Figure 8. The speeding behavior observed warrants further investigation through path analysis (next section). When speeding coincides with risky maneuvers, it can increase user instability, raising the risk of falls or loss of control during interactions with other users. This can lead to potential conflicts, especially in situations where users cross paths or perform overtaking maneuvers.

Path Analysis

Comparing Curve Sites R4 and R7 reveals notable differences in user behavior and conflict risk attributed to changes in curve geometry and the type of bike lane (sidewalk or protected). At R4, where the radius is 6 m and the degree of curvature is 278 degrees, the majority of left-turn users cut the curve while most right-turn users correct their paths. Both types of users frequently pass through the opposite lane. This occurs in a condition where the bike lane is on the sidewalk, allowing users to take more aggressive maneuvers since there is no barrier to stop them, indicating a higher potential for conflict in this sharper curve. In contrast, at R7, where the radius increases to 10 m and the degree of curvature decreases to 178 degrees, users are mostly passing through the central segments. Most right-turn users cut and swing the curve, which increases the risk of potential conflicts. Meanwhile, left-turn users in R7 tend to drift through the central segment.

Figure 11 presents example track typology pie charts for curve sites R4 and R7. It shows how the reduction in curve sharpness at R7 affects track patterns and the associated risks of conflicts. The pie charts reveal that left-turns exhibit more diversity in track-segment types, with up to 12 different types observed. In comparison, right-turns show a maximum of five different types, with the majority involving cutting, correcting, and swinging. This suggests that left-turn users have a wider range of track patterns, indicating that regardless of user type and geometry, users moving outside the curve are more likely to maneuver with large variance.

With reference to the impact of user type (e-scooter versus bike), as mentioned earlier, the frequent track-segment does not show significant variance. However, it is apparent that in a sharper curve, e-scooters maneuver with less type-variance compared with bikes, whereas when the curve gets wider (R7), this trend reverses. This indicates that e-scooters tend to have more consistent behavior in tighter curves but become more variable in wider curves, while bikes exhibit the opposite pattern. The difference in maneuvering patterns between e-scooters and bikes, especially in varying curve geometries, underscores the need for tailored infrastructure designs to accommodate the distinct behaviors and ensure safety for all users.

The analysis of user behavior and conflict risk across the remaining curve sites reveals similar patterns to those observed in earlier sections. At R8, characterized by a flat radius of 22 m and low curvature (78 degrees), both left-turn and right-turn users frequently exhibit drifting maneuvers (DR), passing through all segments of OPL, CL, LN, and OTL. Moving to R9, which is the flattest curve site with a radius of 78 m, users not only exhibit drifting but also frequent swinging maneuvers, with CL segments being the most frequently passed through. At R1 and R2, with the lowest radii of 2 and 5 m, respectively, patterns similar to those observed at R3 and R4 are apparent. Track patterns become more consistent, particularly with left-turn users demonstrating a higher occurrence of cutting maneuvers while touching the opposite lane (CT_OPL). A major difference between R1 and R2 is observed among right-turn users. At the lower radius site (R1), users tend to cut the curve, whereas at R2, users frequently correct their maneuvers outside the bike lane, even though the bike lane is protected. In fact, these users often leave the bike lane at the curve. Sites R3 and R5 exhibit significantly similar patterns, with left-turn users frequently engaging in cutting maneuvers (CT_OPL). However, for right-turn users, a combination of various maneuvers is apparent, with drifting, correcting, and swinging being the most frequent. These findings emphasize the necessity for tailored infrastructure designs that accommodate varying user behaviors and ensure safety across different curve geometries.

To gain a comprehensive understanding of user behavior across all sites, an occurrence heatmap was developed (Figure 12). A quick glance at the heatmap reveals that cutting maneuvers passing through the opposite lane (CT-OPL) are the most prevalent among the sharper curves (R1-R6). This indicates a higher propensity for users to cross into opposing lanes in these areas, suggesting a greater potential for conflicts. Additionally, drifting and correcting maneuvers are the most frequent among left-turn users at site R7 and right-turn users at site R2. This trend indicates that as the curve becomes sharper (with R2 having a radius of 5 m), the direction of the turn significantly influences maneuvering patterns. Specifically, sharper curves appear to compel users to adjust their paths more aggressively, with distinct differences in behavior observed between left and right turns. These findings underscore the importance of considering turn direction and curve sharpness in the design of bike lane infrastructure to enhance user safety and reduce conflict risks.

The clustering analysis resulted in five distinct clusters (0, 1, 2, 3, 4) with an additional group of outliers labeled

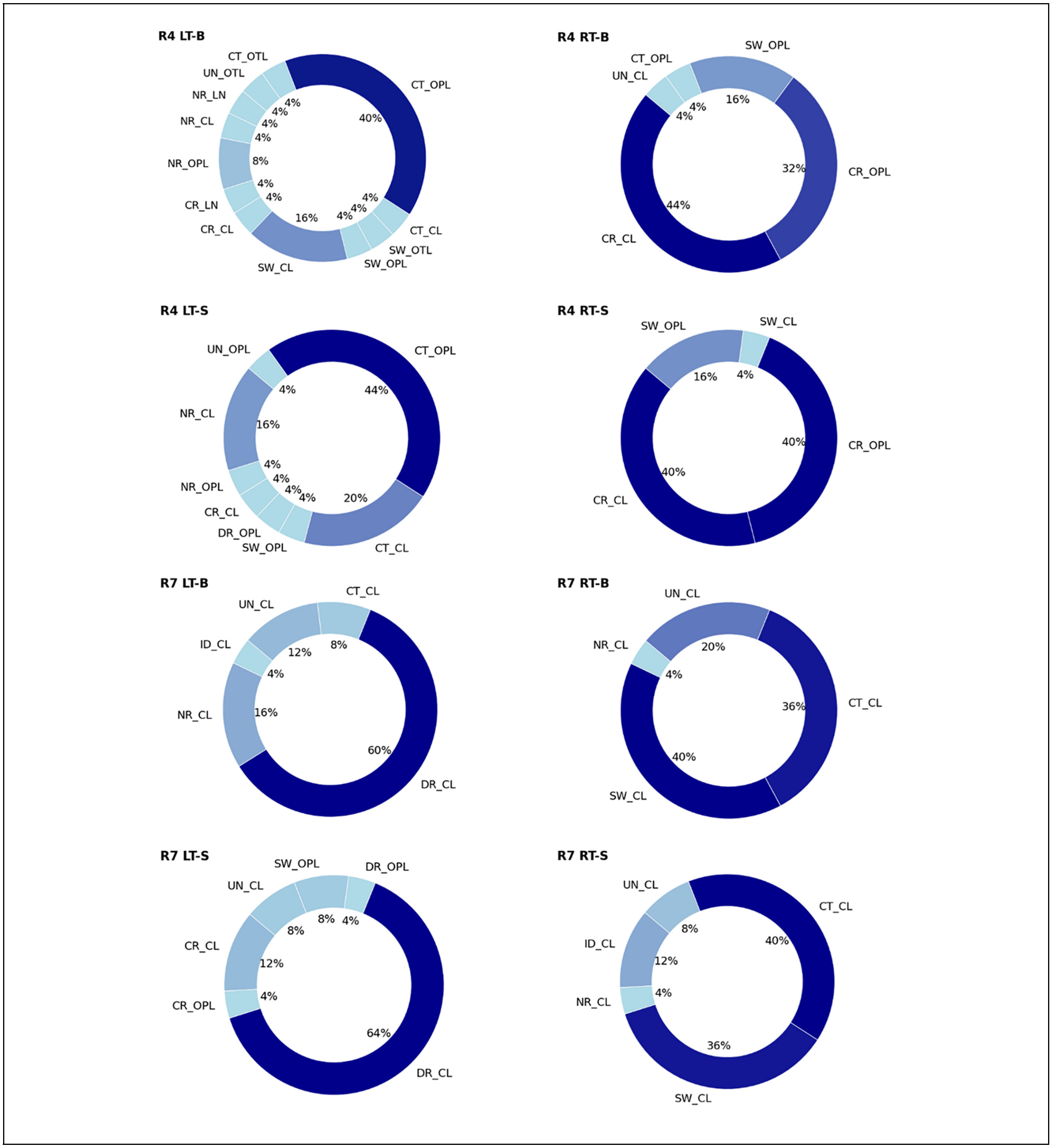

Figure 11. Track-segment occurrence on curve sites R4 = 6 m and R7 = 178 m by user type and direction.
Note: see Table 2 for definition of abbreviations.

as −1. Each cluster represents a unique pattern of lateral offsets (d) at each section of interests (PC, MP, PT) across track paths of bike lane users during curve navigation:

- Cluster 0 (Cutting): This cluster is the largest, with 757 data points. It has a mean d-PC of 26.88, suggesting a slight offset to the right in section PC, and small mean values for d-MP (6.84) and d-PT

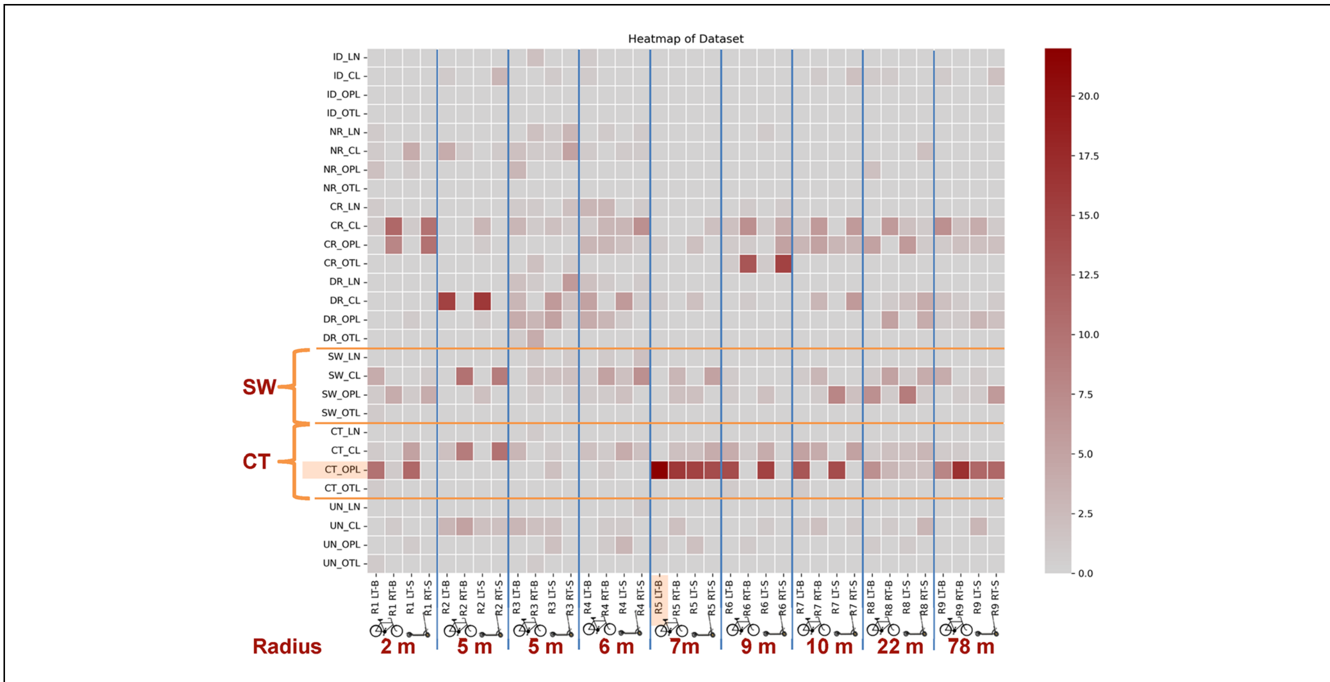

Figure 12. Track-segment occurrence on all nine-curve sites (R1–R9) by user type and direction.
Note: SW = swinging; CT = cutting; see Table 2 for other abbreviations.

(11.05). The standard deviations indicate a moderate spread in these values, especially for d-MP and d-PT, suggesting variability in the offsets in these sections.

- Cluster 1 (Correcting): This small cluster contains eight data points and shows large negative mean values for d-PC (−150.25) and d-MP (−156.13), indicating significant offsets to the left in these sections. The mean d-PT is also negative (−114.63), reinforcing the leftward trend across all sections. The relatively low standard deviations suggest consistency in these offsets.
- Cluster 2 (Correcting): Comprising seven data points, this cluster also shows large negative offsets for d-PC (−112.43) and d-MP (−167.57), but a positive mean d-PT (31.71), indicating a rightward offset in section PT. This cluster exhibits moderate spread, with standard deviations reflecting some variability.
- Cluster 3 (Swinging): With 22 data points, this cluster has negative mean values for d-PC (−82.82) and d-MP (−112.13), suggesting leftward offsets, and a negative mean d-PT (−114.32). The standard deviations show moderate variability, especially for d-MP.
- Cluster 4 (Drifting): The smallest cluster, with only four data points, shows significant negative mean values for d-PC (−153.5) and d-MP (−98.25), indicating strong leftward offsets. However, the mean d-PT is positive (12.5), suggesting a rightward offset in section PT. This cluster has low standard deviations, indicating very consistent offsets.
- Outliers (−1): This group contains 102 data points and is characterized by highly variable offsets, as indicated by the large standard deviations across all sections. These points do not fit well into any of the identified clusters and represent atypical track conditions or measurement anomalies.

To map out various factors influencing track type classifications, a decision tree regression was developed. The results of the regression analysis demonstrated that the degree of curvature is the most significant variable. The resulted decision tree regression plot is shown in Figure 13. In total, 11 predictors existed in the initial data set. These predictors were unmerged and grouped into distinct leaves based on their importance and value ranges. In the resulting tree, it is evident that the variables “user type” and “length of the curve” are not included, indicating they have no impact on the model’s predictions. The top leaf identifies degree of curvature as the primary predictor. The second level is consisted of two leaves of bike lane type (protected or not) and midpoint speed (V_{MP}). In the third level four leaves are identified and predictors include direction, V_{MP}, and V_{PC}. The fourth and fifth levels categorize predictors like chord, V_{PT}, V_{MP}, V_{PC}, and direction within specific ranges. These segments illustrate

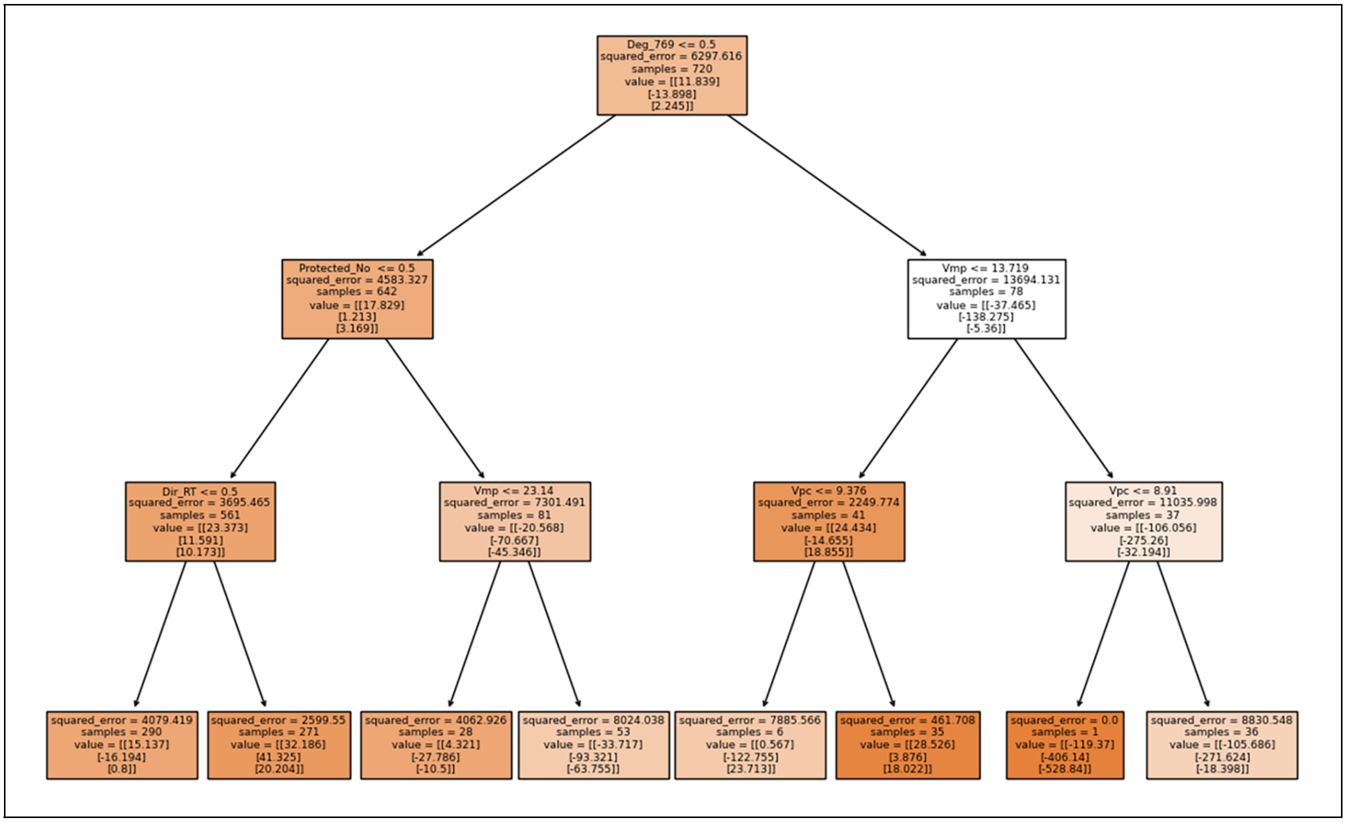

Figure 13. Decision tree regression model visualization showing feature splits for predicting variables d-PC, d-MP, and d-PT.
Note: V_{MP} = midpoint speed; V_{PT} = point of tangency speed V_{PC} = point of curvature speed.

how the decision tree prioritizes and categorizes predictors, revealing their impact on predicting variables d-PC, d-MP, and d-PT with clarity and structure. The best cross-validated score of 62.63 indicates the model's performance in predicting unseen data, with RMSE values of 56.31 for d-PC, 64.37 for d-MP, and 57.48 for d-PT, suggesting moderate prediction accuracy, with d-MP posing the greatest challenge among the target variables. The moderate prediction score in this model suggests the need to replicate the study in the future using a larger data set to improve accuracy and reliability. Achieving this will require the availability or collection of additional video data across more sites with similar and varied geometries, as well as the development of more accurate object-tracking algorithms (e.g., YOLO) to streamline motion extraction with an acceptable level of accuracy.

Discussion

Beyond the new segmentation and classification approach proposed in this study, an effort was made to understand the behavior of 900 micromobility users navigating nine geometrically diverse isolated horizontal curves on bike lanes, an area previously underexplored in the micromobility literature. In this context, four proposed lateral segmentation zones and the cross-sectional LD of micromobility users were used to identify common curve navigation maneuvering patterns, which had been previously introduced in the literature, and to classify users' maneuvering typology during curvature. A key result of this study, valuable for safety practitioners, is the track typology occurrence heatmap (Figure 12), which provides an overview of risky maneuvers observed across various curves, user types, and turning directions. This approach also enabled high-resolution speed analysis, comparing different curves with varying geometries and contrasting user types and turning directions for each cross-section of PC, MP, and PT.

The findings are consistent with those of Xu et al. (*11*) on roadways, where risky trajectory adjustments and high-collision zones were found to be linked to the relationship between trajectory and road geometry. They found that inertia causes vehicles to drift toward the outer edge of a curve after a cut, requiring trajectory correction. In this context, excessive correction frequently resulted in unintended entry into the oncoming lane, a pattern also observed in the current research on bike lane curves. Additionally, Xu et al. (*11*) similarly identified that a smaller horizontal curve radius was found to increase the frequency of trajectory encroachment into opposing traffic lanes. However, it is important to note a key difference between motor vehicles and micromobility devices: the latter have a greater steering angle and smaller body width, which provides them with increased maneuverability (*55*). Additionally, the leaning or lateral inclination of micromobility devices significantly affects trajectory formation, often producing zigzag patterns instead of a smooth arc as a result of their unique physical dynamics. As a result, LD or displacement serves as a valuable criterion for approximating maneuver tracks. This approach streamlines data preparation and facilitates the detection of risky maneuvers by combining track typology analysis with cross-sectional lateral segment observation.

Another finding consistent with previous research is that the degree of curvature is the primary predictor of LD in micromobility users' trajectories on curves. As noted in the introduction, Chen et al. (*12*) also identified horizontal curvature at the current road segment as a significant factor influencing trajectory patterns and lane departures. Davidse et al. (*56*) found that unexpected sharp curves on roads often contribute to increased instability and a higher risk of crashes. Similarly, Afghari et al. (*5*) investigated road users' perceptions of horizontal curves and concluded that lower road predictability in these areas significantly raises the likelihood of crashes. This study supports those findings, but in the context of bike lanes. When many micromobility users tend to cut sharper curves while maintaining speed in free riding conditions, it suggests a repeating pattern that may lead to instability. This risk is heightened when environmental factors, such as surface skid resistance, are lower or when cyclists interact with users coming from the opposite direction.

This study builds on previous research on road curves by introducing a practical approach for assessing the real track typology of micromobility users on bike lane curves. However, a key limitation of the study was the lack of access to pre-existing video data for bike lanes, which required the collection of new data. Additionally, filtering out accurate motion data using Kinovea software was a time-consuming process. The findings are interesting for the design of bike lanes, although they are not conclusive. Although nine curve sites with varied geometric characteristics were analyzed, along with the trajectories of 900 micromobility users, a more robust analysis requires a larger sample size. Future studies should incorporate both real-world observations and controlled experimental studies on predesigned test tracks.

The choice of decision tree regression in this study was motivated by its high interpretability, allowing clear visualization of predictor importance and threshold effects (*57*). This was essential as a first step in understanding how geometric and behavioral variables influence the LD of micromobility users. Its simplicity made it particularly suitable for this initial exploratory analysis with a moderate-sized data set and for communicating intuitive results to practitioners. However, when larger operational data sets become available, future research could benefit from incorporating Random Forest (*58*). This method can improve predictive accuracy and reduce overfitting by averaging the results of multiple decision trees. It is better equipped to capture complex nonlinear relationships and enhances model robustness against variability in user behavior (*58*).

Conclusions

This study investigated the effects of bike lane curve geometry on user behavior while navigating curves, specifically focusing on trajectory, speed, and maneuvering patterns. These behaviors highlight the diverse ways in which cyclists and e-scooter riders navigate curves, influenced by both conscious decisions and unconscious adjustments to the bike lane's geometry. Understanding these patterns provides valuable insights into micromobility users' interactions with infrastructure, which can inform improvements for safety and efficiency. The primary focus of this research was a nonconflict analysis of safety, aimed at identifying risky maneuvers that could increase user instability, particularly concerning single-user accidents. Consequently, only users traveling under free-flow conditions, without the influence of opposing traffic or pedestrians, were included in this analysis. According to Hyden's safety pyramid, a Swedish safety technique, the lowest level observed in proactive safety analysis consists of unsafe acts, which include individual maneuvers that can jeopardize user stability.

The findings demonstrate that the geometry of horizontal curves has a substantial impact on maneuvering behavior. Spatial analysis revealed that left-turn users frequently navigate near the central marking, increasing their vulnerability to cross-lane conflicts. Additionally, a significant proportion of users were observed in the opposite lane at the midpoint of curves, highlighting areas prone to potential conflicts. Speed analysis indicated that higher speeds, particularly on sharper curves, contribute to increased risk and variability in user behavior. E-scooters exhibited higher speeds and greater variability compared with bikes, emphasizing the need for tailored safety measures. The DBSCAN algorithm identified five distinct patterns of lateral offsets, with the largest cluster (84% of users, or 757 individuals) associated with cutting maneuvers that pass through the central lane region, posing side-conflict risks with opposing users.

Predictive modeling through decision tree regression revealed that the degree of curvature is the most influential predictor of user behavior, though the model's moderate prediction accuracy suggests opportunities for further refinement. Notably, sharper curves were found to significantly challenge user stability and safety, with left-turn users often cutting curves and right-turn users correcting their paths, particularly in the absence of physical barriers. These behaviors illustrate that the sharper or more unexpected the curve, the more aggressive and unpredictable the user behavior. Therefore, it is recommended that designers avoid nonstandard curves with radii below 5 m, as well as curves with radii below 10 m on bidirectional bike lanes, as these sharp turns trigger excessive cutting maneuvers, lane violations, and speeding, all of which heighten the risks of instability, falls, and loss of control during interactions. For curves with radii between 5 and 10 m, lane widening at the midpoint and implementing speed-control signage are advised to enhance safety during curvature. E-scooters and bikes displayed differing behaviors on sharp versus flatter curves, and heatmap analysis indicated that cutting maneuvers are most frequent on sharper curves, highlighting higher conflict risks. These results underscore the importance of designing bike lanes that accommodate diverse user behaviors and curve geometries to enhance safety. Future research can explore optimized curvature radii using simulation methods or experimental test tracks to model user perceptions and behaviors under varied scenarios.

Acknowledgments

The authors thank the Municipality of Valencia for granting permission to collect video data on the bike lane network from September to November 2023.

Author Contributions

The authors confirm contribution to the paper as follows: study conception and design: M. Hossein Sabbaghian, D. Llopis-Castelló, A. García; data collection: M. Hossein Sabbaghian; analysis and interpretation of results: M. Hossein Sabbaghian, D. Llopis-Castelló; draft manuscript preparation: M. Hossein Sabbaghian, D. Llopis-Castelló, A. García. All authors reviewed the results and approved the final version of the manuscript.

Declaration of Conflicting Interests

The authors declared no potential conflicts of interest with respect to the research, authorship, and/or publication of this article.

Funding

The authors disclosed receipt of the following financial support for the research, authorship, and/or publication of this article: This research is part of the esMICROMOBILITY research project PID2019-111744RB-I00, funded by MCIN/AEI/10.13039/501100011033.

ORCID iDs

Morteza Hossein Sabbaghian https://orcid.org/0000-0002-2810-3293
David Llopis-Castelló https://orcid.org/0000-0002-9228-5407
Alfredo García https://orcid.org/0000-0003-1345-3685

References

1. Tranter, P., and R. Tolley. *Slow Cities: Conquering Our Speed Addiction for Health and Sustainability*. Elsevier, Amsterdam, the Netherlands, 2020.
2. Chang, S. K. J., and A. F. Ferreira. Bike-Sharing System: Uncovering the "Success Factors." In *International Encyclopedia of Transportation* (R. Vickerman, ed.), Elsevier, Oxford, pp. 355–362, 2021.
3. Harkin, A. M., A. Mangold, K. A. Harkin, and T. Petzoldt. Implicit Communication in Cyclist-Vehicle Interaction: Examining the Influence of Driving Dynamics in Interactions with Turning (Automated) Vehicles on Cyclists' Perceived Safety, Behavioral Intention, and Risk Anticipation. *Journal of Cycling and Micromobility Research*, Vol. 2, 2024, P. 100028. https://doi.org/10.1016/j.jcmr.2024.100028.
4. Bjørnskau, T., K. Karlsen, R. Ingebrigtsen, I. Hesjevoll, K. V. Weyde, and O. Mjåland. ReCyCLIST – A New Powerful Tool to Register and Locate Bicycle and E-Scooter Accidents. *Proc., 11th International Cycling Safety Conference*, November 15–17, 2023, The Hague, the Netherlands, SWOV Institute for Road Safety Research, pp. 126–128. https://swov.nl/sites/default/files/bestanden/downloads/ICSC2023_Book_of_abstracts.pdf. Accessed July 23, 2024.
5. Afghari, A. P., J. Vos, H. Farah, and E. Papadimitriou. "I Did Not See That Coming": A Latent Variable Structural Equation Model for Understanding the Effect of Road Predictability on Crashes along Horizontal Curves. *Accident Analysis & Prevention*, Vol. 187, 2023, P. 107075. https://doi.org/10.1016/j.aap.2023.107075.
6. López-Molina, M., D. Llopis-Castelló, A. M. Pérez-Zuriaga, C. Alonso-Troyano, and A. García. Skid Resistance Analysis of Urban Bike Lane Pavements for Safe Micromobility. *Sustainability*, Vol. 15, No. 1, 2022, p. 698.
7. Jacob, B., and E. Violette. Vehicle Trajectory Analysis: An Advanced Tool for Road Safety. *Procedia-Social and Behavioral Sciences*, Vol. 48, 2012, pp. 1805–1814.
8. Thomas, I. L., and W. T. Taylor. Effect of Edge Striping on Traffic Operations. *Highway Research Board Bulletin*, Vol. 244, 1960, pp. 11–15.
9. Glennon, J. C., and G. D. Weaver. Highway Curve Design for Safe Vehicle Operations. *Highway Research Record*, Vol. 390, 1972, pp. 15–26.
10. Glennon, J. C., and G. D. Weaver. *The Relationship of Vehicle Paths to Highway Curve Design*. Texas Transportation Institute College Station, 1971.

11. Xu, J., X. Luo, and Y.-M. Shao. Vehicle Trajectory at Curved Sections of Two-Lane Mountain Roads: A Field Study under Natural Driving Conditions. *European Transport Research Review*, Vol. 10, No. 1, 2018, P. 12. https://doi.org/10.1007/s12544-018-0284-x.
12. Chen, Y., M. Quddus, and X. Wang. Impact of Combined Alignments on Lane Departure: A Simulator Study for Mountainous Freeways. *Transportation Research Part C: Emerging Technologies*, Vol. 86, 2018, pp. 346–359. https://doi.org/10.1016/j.trc.2017.11.010.
13. Haasnoot, J., R. Happee, V. Van Der Wijk, and A. L. Schwab. Validation of a Novel Bicycle Simulator with Realistic Lateral and Roll Motion. *Vehicle System Dynamics*, Vol. 62, No. 7, 2024, pp. 1802–1826. https://doi.org/10.1080/00423114.2023.2264418.
14. Hossein Sabbaghian, M., D. Llopis-Castelló, and A. García. A Safe Infrastructure for Micromobility: The Current State of Knowledge. *Sustainability*, Vol. 15, No. 13, 2023, p. 10140.
15. Groot, R. *Design Manual for Bicycle Traffic*. CROW, Ede, The Netherlands, 2007.
16. Ul-Abdin, Z., S. Z. Rajper, K. Schotte, P. De Winne, and H. De Backer. Analytical Geometric Design of Bicycle Paths. *Proceedings of the Institution of Civil Engineers - Transport*, Vol. 173, No. 6, 2020, pp. 361–379. https://doi.org/10.1680/jtran.17.00162.
17. Hossein Sabbaghian, M., D. Llopis-Castelló, and A. García. Assessing Micromobility Safety on Horizontal Curves of Bike Lanes: A Video Motion Analysis Methodology. *Traffic Safety Research*, Vol. 7, 2024, p. e000057.
18. Bos, L., M. A. Slawinski, R. A. Slawinski, and T. Stanoev. Modelling of a Cyclist's Power for Time Trials on a Velodrome. *Sports Engineering*, Vol. 27, No. 1, 2024, P. 9. https://doi.org/10.1007/s12283-024-00451-x.
19. Nee, P. J., and J. G. Herterich. Modelling Road Cycling as Motion on a Curve. *Sports Engineering*, Vol. 25, No. 1, 2022, P. 12. https://doi.org/10.1007/s12283-022-00376-3.
20. Shen, X., D. Huang, P. Li, and N. Xu. Trajectory Super-Resolution Methods. In *Handbook of Mobility Data Mining* (H. Zhang, ed.), Amsterdam, Netherlands; Oxford, England; Cambridge, Massachusetts, Elsevier, 2023, pp. 139–156.
21. Zakhem, M., and J. Smith-Colin. Micromobility Implementation Challenges and Opportunities: Analysis of e-Scooter Parking and High-Use Corridors. *Transportation Research Part D: Transport and Environment*, Vol. 101, 2021, P. 103082. https://doi.org/10.1016/j.trd.2021.103082.
22. Pellicer-Chenoll, M., M. Pans, R. Seifert, E. López-Cañada, X. García-Massó, J. Devís-Devís, and L.-M. González. Gender Differences in Bicycle Sharing System Usage in the City of Valencia. *Sustainable Cities and Society*, Vol. 65, 2021, P. 102556. https://doi.org/10.1016/j.scs.2020.102556.
23. Cubells, J., C. Miralles-Guasch, and O. Marquet. Gendered Travel Behaviour in Micromobility? Travel Speed and Route Choice through the Lens of Intersecting Identities. *Journal of Transport Geography*, Vol. 106, 2023, P. 103502. https://doi.org/10.1016/j.jtrangeo.2022.103502.
24. Fabregat Bosch, J. *Detection & Tracking for Micromobility Safety Using Computer Vision and Artificial Intelligence*. Bachelor thesis. Universitat Politècnica de Catalunya, Spain, 2020.
25. Sanders, T., and E. Karpinski. Implications for Interactions between Micromobility and Autonomous Vehicles. *SAE International Journal of Connected and Automated Vehicles*, Vol. 6, No. 2, 2022, pp. 185–197. https://doi.org/10.4271/12-06-02-0012.
26. Sanjurjo-de-No, A., A. María Pérez-Zuriaga, C. Hortelano, and A. García. Analyzing Micromobility Patterns: A Gender Perspective on Behavior and Risk Perception. *Transportation Research Part F: Traffic Psychology and Behaviour*, Vol. 109, 2025, pp. 1365–1382. https://doi.org/10.1016/j.trf.2025.01.044.
27. Spacek, P. Track Behavior in Curve Areas: Attempt at Typology. *Journal of Transportation Engineering*, Vol. 131, No. 9, 2005, pp. 669–676. https://doi.org/10.1061/(ASCE)0733-947X(2005)131:9(669).
28. Bharat Kumar Anna, V. A., S. P. Venthuruthiyil, and M. Chunchu. Vehicle Trajectory Data Extraction from the Horizontal Curves of Mountainous Roads. *Transportation Letters*, Vol. 15, No. 9, 2023, pp. 1055–1065. https://doi.org/10.1080/19427867.2022.2125487.
29. Mauriello, F., A. Montella, M. Pernetti, and F. Galante. An Exploratory Analysis of Curve Trajectories on Two-Lane Rural Highways. *Sustainability*, Vol. 10, No. 11, 2018, P. 4248. https://doi.org/10.3390/su10114248.
30. MacQueen, J. Some Methods for Classification and Analysis of Multivariate Observations. Proceeding of 5th Berkeley Symposium on Mathematocal Statistics and Probability, No. 1, 1967, pp. 281–297.
31. Hartigan, J. A., and M. A. Wong. Algorithm AS 136: A K-Means Clustering Algorithm. *Journal of the Royal Statistical Society. Series C (Applied Statistics)*, Vol. 28, No. 1, 1979, pp. 100–108. https://doi.org/10.2307/2346830.
32. Xu, X., M. Ester, H.-P. Kriegel, and J. Sander. Clustering and Knowledge Discovery in Spatial Databases. *Vistas in Astronomy*, Vol. 41, No. 3, 1997, pp. 397–403. https://doi.org/10.1016/S0083-6656(97)00044-5.
33. Fraley, C., and A. E. Raftery. Enhanced Model-Based Clustering, Density Estimation, and Discriminant Analysis Software: MCLUST. *Journal of Classification*, Vol. 20, No. 2, 2003, pp. 263–286. https://doi.org/10.1007/s00357-003-0015-3.
34. Cleveland, W. S. Robust Locally Weighted Regression and Smoothing Scatterplots. *Journal of the American Statistical Association*, Vol. 74, No. 368, 1979, pp. 829–836. https://doi.org/10.1080/01621459.1979.10481038.
35. Friedman, J. H. Multivariate Adaptive Regression Splines. *The Annals of Statistics*, Vol. 19, No. 1, 1991, pp. 1–67.
36. Cortes, C., and V. Vapnik. Support-Vector Networks. *Machine Learning*, Vol. 20, 1995, pp. 273–297.
37. Foresee, F. D., and M. T. Hagan. Gauss-Newton Approximation to Bayesian Learning. *Proc., International Conference on Neural Networks (ICNN'97)*, Houston, TX, IEEE, New York, NY, Vol. 3, 1997, pp. 1930–1935.
38. Quinonero-Candela, J., and C. E. Rasmussen. A Unifying View of Sparse Approximate Gaussian Process Regression.

The Journal of Machine Learning Research, Vol. 6, 2005, pp. 1939–1959.

39. Mohammed, H., A. Y. Bigazzi, and T. Sayed. Characterization of Bicycle Following and Overtaking Maneuvers on Cycling Paths. *Transportation Research Part C: Emerging Technologies*, Vol. 98, 2019, pp. 139–151. https://doi.org/10.1016/j.trc.2018.11.012.
40. Prati, G., F. Fraboni, M. De Angelis, L. Pietrantoni, D. Johnson, and J. Shires. Gender Differences in Cycling Patterns and Attitudes toward Cycling in a Sample of European Regular Cyclists. *Journal of Transport Geography*, Vol. 78, 2019, pp. 1–7. https://doi.org/10.1016/j.jtrangeo.2019.05.006.
41. Gioldasis, C., Z. Christoforou, and R. Seidowsky. Risk-Taking Behaviors of e-Scooter Users: A Survey in Paris. *Accident Analysis & Prevention*, Vol. 163, 2021, P. 106427. https://doi.org/10.1016/j.aap.2021.106427.
42. Cabrera, F., and A. Sofía. Caracterización de la maniobra de adelantamiento y el comportamiento frente al tráfico opuesto de los usuarios de vehículos de movilidad personal mediante el uso de un patinete eléctrico instrumentado con tecnología Raspberry Pi. Aplicación práctica en el distrito Algirós de la ciudad de Valencia, Universitat Politècnica de València, Valencia, Spain, 2021. https://riunet.upv.es/handle/10251/175929.
43. Organismo Autónomo Centro Nacional de Información Geográfica. Centro de Descargas Del CNIG (IGN). *Centro de Descargas del CNIG*. http://centrodedescargas.cnig.es. Accessed July 24, 2024.
44. Google Maps. *7 Av. de Aragón*. https://www.google.es/maps/place/39%C2%B028'11.2%22N + 0%C2%B021'35.0%22W/@39.469774,-0.3603732,212m/data = !3m2!1e3!4b1!4m4!3m3!8m2!3d39.469773!4d-0.3597295?entry = ttu&g_ep = EgoyMDI1MDMxOS4yIKXMDSoASAFQAw%3D%3D. Accessed March 24, 2025.
45. Google Maps. *1 C/ Angel Guimera*. https://www.google.es/maps/place/39%C2%B028'13.1%22N + 0%C2%B023'00.9%22W/@39.4703097,-0.3861582,846m/data = !3m2!1e3!4b1!4m4!3m3!8m2!3d39.4703056!4d-0.3835833?entry = ttu&g_ep = EgoyMDI1MDMxOS4yIKXMDSoASAFQAw%3D%3D. Accessed March 24, 2025.
46. Google Maps. *C. de Alicante*. https://www.google.es/maps/place/39%C2%B028'02.5%22N + 0%C2%B022'36.3%22W/@39.4673652,-0.3793249,846m/data = !3m2!1e3!4b1!4m4!3m3!8m2!3d39.4673611!4d-0.37675?entry = ttu&g_ep = EgoyMDI1MDMxOS4yIKXMDSoASAFQAw%3D%3D. Accessed March 24, 2025.
47. Google Maps. *177 Avda. de Blasco Ibáñez*. https://www.google.es/maps/place/39%C2%B028'14.9%22N + 0%C2%B020'08.7%22W/@39.4707094,-0.3357818,106m/data = !3m1!1e3!4m4!3m3!8m2!3d39.4708101!4d-0.3357394?entry = ttu&g_ep = EgoyMDI1MDMxOS4yIKXMDSoASAFQAw%3D%3D. Accessed March 24, 2025.
48. Google Maps. *175 Avda. de Blasco Ibáñez*. https://www.google.es/maps/place/39%C2%B028'14.2%22N + 0%C2%B020'08.8%22W/@39.4706114,-0.3355738,53m/data = !3m1!1e3!4m4!3m3!8m2!3d39.470618!4d-0.335771?entry = ttu&g_ep = EgoyMDI1MDMxOS4yIKXMDSoASAFQAw%3D%3D. Accessed March 24, 2025.
49. Google Maps. *Valencia Cabanyal*. https://www.google.es/maps/@39.470249,-0.3349849,212m/data = !3m1!1e3?entry = ttu&g_ep = EgoyMDI1MDMxOS4yIKXMDSoASAFQAw%3D%3D. Accessed March 24, 2025.
50. Google Maps. *Pl. de la Prta del Mar*. https://www.google.es/maps/place/39%C2%B028'18.4%22N + 0%C2%B022'07.2%22W/@39.471725,-0.3689401,53m/data = !3m1!1e3!4m4!3m3!8m2!3d39.4717778!4d-0.3686667?entry = ttu&g_ep = EgoyMDI1MDMxOS4yIKXMDSoASAFQAw%3D%3D. Accessed March 24, 2025.
51. Google Maps. *Penya-Roja*. https://www.google.es/maps/place/39%C2%B027'36.0%22N + 0%C2%B021'15.2%22W/@39.4599607,-0.3545399,63m/data = !3m1!1e3!4m4!3m3!8m2!3d39.46!4d-0.3542222?entry = ttu&g_ep = EgoyMDI1MDMxOS4yIKXMDSoASAFQAw%3D%3D. Accessed March 24, 2025.
52. Google Maps. *7 Av. del Professor López Piñero*. https://www.google.es/maps/@39.4538299,-0.3526517,53m/data = !3m1!1e3?entry = ttu&g_ep = EgoyMDI1MDMxOS4yIKXMDSoASAFQAw%3D%3D. Accessed March 24, 2025.
53. NYC DOT Web page. Two-Way Bike Lane and NYC Street Design Manual. https://www.nycstreetdesign.info/geometry/two-way-bike-lane. Accessed May 31, 2024.
54. Kononenko, I., and M. Kukar. Cluster Analysis. In *Machine Learning and Data Mining* (I. Kononenko, and M. Kukar, eds.), Woodhead Publishing, Cambridge, UK, 2007, pp. 321–358. https://doi.org/10.1533/9780857099440.321.
55. Hossein Sabbaghian, M. *Developing a Comprehensive Methodology to Improve Geometric Design and Safety in Micromobility Infrastructure*. PhD thesis. Universitat Politècnica de València, Spain, 2024.
56. Davidse, R. J., K. V. Duijvenvoorde, and W. J. R. Louwerse. *Fatal Road Crashes on National Roads in 2019; Analysis of Crash and Injury Factors and Resulting Potential Countermeasures*. SWOV, Leidschendam, the Netherlands, 2020.
57. Liu, Z., Z. Gu, and P. Liu. Decision Tree. In *Transportation Big Data* (Z. Liu, Z. Gu, and P. Liu, eds.), Elsevier, Amsterdam, Netherlands, 2024, pp. 247–285. https://doi.org/10.1016/B978-0-443-33891-5.00015-6.
58. Belgiu, M., and L Drăguţ. Random Forest in Remote Sensing: A Review of Applications and Future Directions. *ISPRS Journal of Photogrammetry and Remote Sensing*, Vol. 114, 2016, pp. 24–31. https://doi.org/10.1016/j.isprsjprs.2016.01.011.